Dilute resonant scatterers in a parabolic band: Density of states as a function of scattering strength

A. P. Jauho
Nordisk Institut for Teoretisk Atomfysik (NORDITA), Blegdamsvej 17, DK-2100 Copenhagen Ø, Denmark

J. W. Wilkins
Laboratory of Atomic and Solid State Physics, Cornell University, Ithaca, New York 14853
(Received 15 March 1983)

The model of dilute resonant scatterers in a constant—density-of-states metal is extended to the case where the conduction band is parabolic as is the case for a semiconductor near its band gap. Within this model a self-consistent formulation of the density of states is evaluated with the use of both standard numerical methods and an analytical integration technique recently proposed for parabolic bands. In the limit of weak scattering the two methods agree reasonably well, but the analytic method fails badly as the scattering strength increases. In the course of the analysis, we (i) develop a coherent-potential approximation for the self-energy, (ii) display densities of states projected both on the localized scattering impurities and on the initial conduction-band states, and (iii) discover that the analytic method implicitly (and necessarily to maintain its simplicity) assumes a zero-range potential and hence cannot lead to an impurity band.

I. INTRODUCTION

The resonant-level model (RLM) [also known as the virtual—bound-state model (VBM)] describes a localized state in a continuum; the conduction electrons make transitions between the localized level and the conduction band thus forming a scattering resonance. By varying the parameters of the model one can adjust the position of the scattering resonance with respect to the Fermi level thus displaying a variety of physical phenomena.

Since its introduction,[1,2] numerous applications for the RLM have been found. These include discussions of residual resistivities due to transition-metal impurities in simple metals,[2] magnetic susceptibilities of virtual—bound-state alloys,[3,4] and static[5] and dynamic[6,7] aspects of chemisorption. Owing to its convenient mathematical properties the RLM has often been employed as a model interaction in cases where an analytic treatment has been desired. As an example, we mention recent studies of high-electric-field quantum transport.[8]

In metal physics it is commonplace to make the so-called constant—density-of-states approximation, i.e., the momentum summations are performed according to the prescription

$$\int \frac{d^3k}{(2\pi)^3} f(\vec{k}) = \int_{-\mu}^{\infty} d\epsilon_k N(\epsilon_k) \int \frac{d\Omega_k}{4\pi} f(\epsilon_k, \hat{k})$$

$$\simeq N(\epsilon_F) \int_{-\infty}^{\infty} d\epsilon_k \int \frac{d\Omega_k}{4\pi} f(\epsilon_k, \hat{k}) , \quad (1)$$

where $f(\vec{k})$ is an arbitrary function of the momentum. Here $N(\epsilon_k)$ is the density of states which, for example, would have a characteristic square-root dependence on energy for free electrons. To our knowledge, until quite recently all work on the RLM has been within the constant—density-of-states approximation. The reason is, of course, the enormous technical complications one might expect to arise from a more realistic choice for the density of states. However, Pankratov[9] has succeeded in carrying out the analysis with the free-carrier density of states $N(\epsilon_k) \sim \sqrt{\epsilon_k}$. Such a density of states occurs near the band gaps of semiconductors in contrast to metals where a constant density of states often is more appropriate. The main technical novelty in Ref. 9 is the application of contour-integration techniques: Use is made of the branch-cut properties of the square-root function arising due to the free-electron density of states.

Unfortunately the final results in Ref. 9 are misleading. The point is that, in the self-consistent determination of the self-energy functional, the author of Ref. 9 arbitrarily truncates the perturbation series after the first two terms. In fact (see Sec. II B), it is possible to carry out the summation exactly to all orders. After this has been done it is interesting to compare how well the results obtained with the analytical technique [which requires a somewhat *ad hoc* cutoff procedure (see Sec. III)] agree with numerical calculations. It is found that in the weak coupling limit the two calculations are in reasonable agreement, whereas in the strong coupling limit the analytical method fails badly in the sense that it can never lead to an isolated impurity band. This failure can be traced precisely to the cutoff procedure implicit in the analytical method.

The organization of this paper is as follows. We first review the technique of impurity averaging as it applies to the resonant-level model. We then introduce the analytical method suggested by Pankratov[9] and apply it to the coherent-potential-approximation (CPA) equations for the self-energy. We present numerical calculations corresponding to the analytical results and conclude by proving that in the Pankratov scheme no isolated impurity bands can arise. An explanation for this behavior is provided.

II. IMPURITY AVERAGING: THE RESONANT-LEVEL MODEL

A. General remarks

The problem is defined by the Hamiltonian

$$H=\sum_{\vec{p}}\epsilon_{\vec{p}}a^{\dagger}_{\vec{p}}a_{\vec{p}}+E\sum_{\alpha}b^{\dagger}_{\alpha}b_{\alpha}+\sum_{\vec{p},\alpha}[V(\vec{p})e^{-i\vec{p}\cdot\vec{R}_{\alpha}}a^{\dagger}_{\vec{p}}b_{\alpha}+V^{*}(\vec{p})e^{i\vec{p}\cdot\vec{R}_{\alpha}}b^{\dagger}_{\alpha}a_{\vec{p}}] . \tag{2}$$

Here $a_{\vec{p}}$ is the destruction operator for an electron in a state $\vec{p}$, and b_{α} is the destruction operator for the localized state at the location $\vec{R}_{\alpha}$. The energy E defines the position of the localized level with respect to the conduction band and $V(\vec{p})$ is the hybridization matrix element between the localized level and the conduction band.

The objective is to calculate the density of states with the formula

$$\rho(\epsilon)=-\frac{1}{\pi}\mathrm{Tr}\,\mathrm{Im}\,\bar{G}(\epsilon) , \tag{3}$$

where $\bar{G}$ is the impurity-averaged retarded Green function.

In the calculation of the Green function we follow the standard procedure: The equation of motion for the Green function is iterated and impurity averaged term by term. Finally, an infinite partial resummation is carried out in order to construct a self-energy functional which can be used in (3). In what follows, we give a rather detailed treatment because this allows the introduction of the notation used in later sections in a convenient way.

B. Construction of the self-energy functional

In this paper we need to consider only the following retarded Green functions:

$$G(\vec{p},\vec{p}\,';t)=-i\Theta(t)\langle\{a_{\vec{p}}(t),a^{\dagger}_{\vec{p}\,'}(0)\}\rangle , \tag{4}$$

$$g(\alpha,\alpha';t)=-i\Theta(t)\langle\{b_{\alpha}(t),b^{\dagger}_{\alpha'}(0)\}\rangle \tag{5}$$

for the conduction electrons and the localized levels, respectively. In (4) and (5) the curly brackets indicate an anticommutator and $\Theta(t)$ is the unit step function. The equation of motion for G is obtained in the standard fashion; after Fourier transforming with respect to time, one obtains the following integral equation for G.

$$G(\vec{p},\vec{p}\,';\epsilon)=\delta_{\vec{p},\vec{p}\,'}G_0(\vec{p},\epsilon)+G_0(\vec{p},\epsilon)V(\vec{p})g_0(\epsilon)\times\sum_{\vec{k},\alpha}e^{-i(\vec{p}-\vec{k})\cdot\vec{R}_{\alpha}}\times V^{*}(\vec{k})G(\vec{k},\vec{p}\,';\epsilon) . \tag{6}$$

In (4) we have used the noninteracting Green functions for the conduction electrons and the localized level, respectively,

$$G_0(\vec{p},\epsilon)=(\epsilon-\epsilon_{\vec{p}}+i\eta)^{-1} , \tag{7}$$

$$g_0(\alpha,\epsilon)=(\epsilon-E+i\eta)^{-1} . \tag{8}$$

Note that before impurity averaging the translational invariance is broken and two momenta are needed to describe the Green function.

The next step is to iterate (6), to average it term by term, and to arrange the result into the form of a diagrammatic perturbation theory. The details can be found, for example, in the review article by Elliot, Krumhansl, and Leath[10]; see especially their Sec. III A 3. It is therefore sufficient to state their main results modified so as to correspond to the resonant-level model.

The simplest possible choice for the self-energy would be the so-called averaged—t-matrix approximation (ATA) where one chooses

$$\Sigma^{\mathrm{ATA}}_{\vec{k}}(\epsilon)=\frac{c[V(\vec{k})]^2}{\epsilon-E-\sum_{\vec{q}}|V(\vec{q})|^2G_0(\vec{q},\epsilon)} . \tag{9}$$

In (9), c denotes the concentration of the resonant impurities. Next, the CPA is obtained by summing the same single-site diagrams as leading to (9) but with the full impurity-averaged Green function inserted self-consistently in the internal lines. The result is

$$\Sigma_{\vec{k}}(\epsilon)=\frac{c[V(\vec{k})]^2}{\epsilon-E-\sum_{\vec{q}}|V(\vec{q})|^2\bar{G}(\vec{q},\epsilon)} . \tag{10}$$

As it stands, (10) implies multiple counting of certain diagrams; this can be corrected by subtracting the multiply counted terms and determining the self-energy from the following self-consistent equation (see Ref. 10 for details and references to the original papers):

$$\Sigma^{\mathrm{CPA}}_{\vec{k}}(\epsilon)=\frac{c[V(\vec{k})]^2}{\epsilon-E-\sum_{\vec{q}}\{[V(\vec{q})]^2-(\epsilon-E)\Sigma^{\mathrm{CPA}}_{\vec{q}}(\epsilon)\}\bar{G}(\vec{q},\epsilon)} . \tag{11}$$

It should be noted that (11) requires rather an involved self-consistent solution because the impurity-averaged Green function appearing in (10) or (11) itself depends on the unknown self-energy via

$$\bar{G}(\vec{q},\epsilon)=[\epsilon-\epsilon_{\vec{q}}-\Sigma_{\vec{q}}(\epsilon)]^{-1} . \tag{12}$$

It would also appear that the momentum dependence of the self-energy might complicate the matters. However, the separable character of the resonant-level interaction facilitates the following simple analysis.

In order to simplify the notation let us introduce

$$A(\epsilon)\equiv\sum_{\vec{k}}[V(\vec{k})]^2\bar{G}(\vec{k},\epsilon) , \tag{13}$$

$$B(\epsilon)\equiv\sum_{\vec{k}}\Sigma_{\vec{k}}(\epsilon)\bar{G}(\vec{k},\epsilon) . \tag{14}$$

Then the self-consistent solution involves the iteration of the following two coupled equations:

$$B(\epsilon)=\frac{cA(\epsilon)}{(\epsilon-E)-A(\epsilon)+(\epsilon-E)B(\epsilon)} , \tag{15}$$

$$A(\epsilon)=\sum_{\vec{q}}\frac{V(\vec{q})^2}{\epsilon-\epsilon_{\vec{q}}-\dfrac{cV(\vec{q})^2}{\epsilon-E-A(\epsilon)+(\epsilon-E)B(\epsilon)}} . \tag{16}$$

Once a convergent solution for (15) and (16) has been found, the self-energy is finally computed from

$$\Sigma_{\vec{q}}(\epsilon)=\frac{c[V(\vec{q})]^2}{\epsilon-E-A(\epsilon)+(\epsilon-E)B(\epsilon)} \equiv[V(q)]^2 g(\epsilon) . \tag{17}$$

In the second part of Eq. (17) we note the connection between the conduction-electron self-energy and the resonant-level propagator $g(\epsilon)$, Eq. (5).

Let us examine now some limiting cases of the above self-energy functionals. For the case $c=1$ the system consists only of resonant levels. Therefore the solution

$$\Sigma_{\vec{k}}^{\mathrm{CPA}}(\epsilon)\,|_{c=1}=\frac{[V(\vec{k})]^2}{\epsilon-E} , \tag{18}$$

which follows from (11) by inspection, leads to the correct expression for $g(\epsilon)$ when substituted in (17).

Next, in the dilute concentration limit $c \ll 1$ the full CPA equation (11) reduces to (10). It should be noted, however, that even (10) contains all powers of the concentration through the self-consistent solution for the impurity-averaged Green function. In what follows we will confine ourselves to the dilute limit. Hence in all our calculations the simplified expression (10) is used.

Pankratov[9] uses in his work the first two terms of the series expansion of (11),

$$\Sigma_{\vec{k}}^{P}(\epsilon)=c[V(\vec{k})]^2 g_0(\epsilon)+c[V(\vec{k})]^2 g_0^2(\epsilon)A(\epsilon) , \tag{19}$$

where the auxiliary quantity $A(\epsilon)$ was defined in (13). This is clearly inadequate: The very nature of the resonant-level model requires an infinite summation of the quantity $g_0(\epsilon)$ in order to build in the resonant form for the imaginary part of the self-energy [see also Eq. (20) below]. It is therefore no surprise that Pankratov's final results involve unphysical features: (i) his "impurity band" vanishes as the interaction is made stronger (which is the opposite to what one expects), and (ii) in the weak coupling limit his result for the density of states does not reduce to a narrow resonance superposed on the unperturbed conduction band (see also Fig. 3).

We conclude this section by pointing out that it is relatively straightforward to solve the self-consistent equations (10) and (12) *within* the constant—density-of-states approximation if one assumes that the momentum dependence of the interaction $V(\vec{k})$ is weak. One obtains as a final result the expected resonant structure for the imaginary part of the self-energy,

$$\mathrm{Im}\Sigma^{\mathrm{RLM}}(\omega)=\frac{c}{\pi N(\epsilon_F)}\frac{\Gamma^2(\epsilon_F)}{(\omega-E)^2+\Gamma^2(\epsilon_F)} , \tag{20}$$

where the level width is given by

$$\Gamma(\epsilon)=\pi N(\epsilon)V^2 , \tag{21}$$

and $N(\epsilon)$ is the density of states for free electrons.

III. ANALYTICAL CALCULATION

In this section we use Pankratov's contour-integration technique to solve the self-consistent problem defined by (10), (12), and (13),

$$A(\epsilon)=\sum_{\vec{q}}\frac{[V(\vec{q})]^2}{\epsilon-\epsilon_{\vec{q}}-\dfrac{c[V(\vec{q})]^2}{\epsilon-E-A(\epsilon)}} . \tag{22}$$

We remind the reader that the choice (10) for the self-energy implies a dilute impurity concentration. We will assume that the interaction $V(\vec{q})$ does not depend on direction so that the integration in (22) can be transformed into an one-dimensional energy integration. We write the interaction $V(\vec{k})$ as $V(\vec{k})=V_0 v(\epsilon_k)$, where V_0 is a strength parameter with units of energy and the form, or range, function $v(\epsilon_k)$ is dimensionless but involves another parameter describing the range of the interaction. Equation (22) is then transformed into

$$a(\omega)=-\frac{2}{\pi}\sqrt{\gamma}\int_0^\infty dy\frac{y^{1/2}v^2(Ey)}{y-(\omega+1)+\delta\dfrac{v^2(Ey)}{\omega-a(\omega)}} , \tag{23}$$

where we have introduced

$$\omega=(\epsilon/E)-1 , \quad a=A/E , \quad \gamma=\left[\frac{\Gamma(E)}{2E}\right]^2=\left[\frac{\pi N(E)V_0^2}{2E}\right]^2 , \quad \delta=cV^2/E^2 . \tag{24}$$

The model is thus defined by three parameters: γ, δ and the as of yet unspecified range parameter. It is interesting to note that the concentration does not appear as an independent parameter because it is involved only through δ. However, had we used the full CPA expression for the self-energy the concentration would appear as an independent parameter.

The integral in (23) converges only if the range function $v(Ey)$ vanishes sufficiently rapidly at infinity. Impurity potentials are often approximated by a screened Coulomb potential for which we have

$$v(Ey)=(1+Ey/E^{\mathrm{scr}})^{-1} , \tag{25}$$

where we explicitly display the range parameter E^{scr}. The form (25) vanishes sufficiently rapidly to make (23) convergent.

In Pankratov's work[9] it is assumed that the interaction is constant "in the important region of integration" and that it vanishes (but in an unspecified way) at infinity. Therefore, Pankratov replaces $v^2(Ey)$ in (23) by unity and treats the now formally divergent integral as convergent. This procedure will, however, lead to severe problems as we shall see below. Here we proceed with the analysis as

indicated by Pankratov.

Define

$$I_C=\int_C dz\frac{z^{1/2}V(z)}{z-D(\omega)}\ , \tag{26}$$

where the contour C is depicted in Fig. 1. We have

$$I_C=I_R+I_-+I_\epsilon+I_+\ . \tag{27}$$

In (23) we need I_+; since I_R and I_ϵ vanish and I_- equals I_+ we get

$$I_+=\pi i\sqrt{D(\omega)}\ , \tag{28}$$

or, going back to (23),

$$a(\omega)=-2i\sqrt{\gamma}\left[\omega+1-\frac{\delta}{\omega-a(\omega)}\right]^{1/2}\ , \tag{29}$$

which can be rearranged to give

$$a^3(\omega)-\omega a^2(\omega)+4\gamma(1+\omega)a(\omega)-4\gamma[\omega(\omega+1)-\delta]=0\ . \tag{30}$$

Now, in principle, one can write down the solutions of this cubic equation but the resulting expressions are quite unwieldy and not particularly useful for extracting qualitative information about the density of states such as the existence or nonexistence of isolated impurity bands for some particular values of the parameters. However, (30) can directly be used to show that the density of states resulting from $a(\omega)$ determined by (30) *cannot* exhibit an isolated impurity band, and we proceed to give such a proof.

Recall first that the density of states vanishes if the quantity $a(\omega)$ is real [see (3)]. Rewrite (30) as

$$\frac{a^2(\omega)}{4\gamma}=-(1+\omega)+\frac{\delta}{\omega-a(\omega)}\ . \tag{31}$$

The question of whether the density of states vanishes or not can now be formulated in terms of a graphical construction. Equation (31) describes a parabola and hyperbola; if these two curves have three intercepts $a(\omega)$ is real and hence the density of states vanishes, whereas if there is only one intercept $a(\omega)$ can be chosen to be complex which leads to a finite density of states. The first situation corresponds to the situation where the cubic equation (30) has three real roots and the second one corresponds to the case where there is one real and two complex roots (which are complex conjugates corresponding to the retarded and advanced Green functions, respectively). Figure 2 shows these curves for two different choices of parameters. We will focus on the right-hand branch of the hyperbola because the left branch always leads to a real $a(\omega)$, i.e., a vanishing density of states. The behavior is now simple indeed: As the energy is increased, the hyperbola moves towards the lower-right-hand corner. At a certain critical energy, the hyperbola passes below the parabola. (In Fig. 2 this happens at about $\omega\sim-1.5$.) Thus (30) possesses complex solutions (which are needed for a finite density of states) only above this critical energy. The center of the hyperbola moves on a straight line when the energy is changed and hence it is not possible for the right-hand branch of the hyperbola to intersect the parabola once it has moved outside of it. Thus it is not possi-

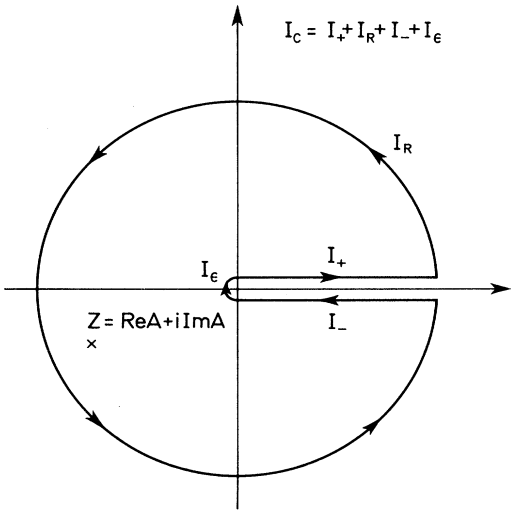

FIG. 1. Contour C introduced by Pankratov. Contribution from the large circle vanishes due to the implicit cutoff in the scattering interaction and the contribution from the small circle vanishes as $\epsilon\to0$. Hence $I_C=I_++I_-=2I_+=2\pi i\times$(sum of residues). The last equality leads to the result (28) used in the text. The branch cut in (26) is placed on the positive x axis. Pole at $z=\mathrm{Re}D(\omega)+i\,\mathrm{Im}D(\omega)$ is placed in the lower half-plane because we are dealing with the retarded function.

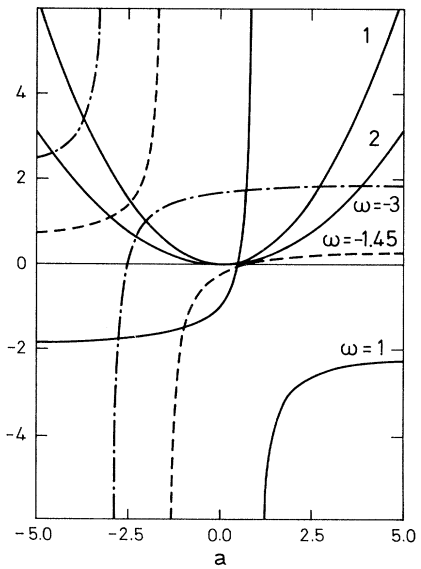

FIG. 2. Graphical representation of (36) for the cases $\gamma=\delta=1$ (curve 1) and $\gamma=2$, $\delta=1$, (curve 2), and for energies $\omega=-3$ (dashed-dotted curve), $\omega=-1.45$ (dashed curve), and $\omega=1$ (solid curve). Allowed energies begin when the hyperbola moves outside the parabola; this occurs at approximately $\omega\sim-1.5$; this value is very closely the same for curves 1 and 2.

ble to have any forbidden regions in the allowed energy domain. In other words, (30) can never lead to an isolated impurity band.

We can understand this behavior as follows.[11] In the Pankratov technique the potential is described basically by one parameter only (i.e., its strength V_0). This situation can be viewed as corresponding to a potential whose Fourier transform is a *constant,* i.e., a zero-range potential. But a three-dimensional δ-function potential cannot support bound states. Therefore, it is not surprising that the Pankratov technique, which implicitly assumes a zero-range potential, does not lead to an impurity band. We will show in the next section densities of states which have been calculated either with the Pankratov technique or by a direct numerical solution of the self-consistent equation (23) with a suitable model interaction.

IV. DENSITIES OF STATES

A. Analytical method

In the Appendix we show that the densities of states are given within the Pankratov technique by

$$\tilde{\rho}^{\,\mathrm{cond}}(\omega)=\frac{\rho^{\,\mathrm{cond}}(\omega)}{N(E)}$$
$$=\frac{1}{\sqrt{2}}(\omega+1-\mathrm{Re}\tilde{\Sigma}(\omega)$$
$$+\{[\omega+1-\mathrm{Re}\tilde{\Sigma}(\omega)]^2+[\mathrm{Im}\tilde{\Sigma}(\omega)]^2\}^{1/2})^{1/2} \tag{32}$$

and

$$\tilde{\rho}^{\,\mathrm{loc}}(\omega)=\frac{1}{2}\frac{\delta}{\sqrt{\gamma}}\frac{\mathrm{Im}a(\omega)}{[\omega-\mathrm{Re}a(\omega)]^2+[\mathrm{Im}a(\omega)]^2}\ , \tag{33}$$

where $\tilde{\rho}^{\,\mathrm{cond}}$ and $\tilde{\rho}^{\,\mathrm{loc}}$ correspond to the conduction electron and localized level components of the density of states, respectively, and $\tilde{\Sigma}(\omega)$ is given by (10),

$$\tilde{\Sigma}(\omega)=\frac{\delta}{\omega-a(\omega)}\ . \tag{34}$$

Numerical applications of (32) and (33) are further discussed in Sec. IV C.

B. Numerical calculations

In order to solve (23) numerically one has to specify the functional form for the range function $v(Ey)$. To achieve a situation which corresponds to Pankratov's case as closely as possible, we present in this paper results for a unit step function form,

$$v(\epsilon_k)=\Theta(D-\epsilon_k)\ . \tag{35}$$

We have tested several values for the energy cutoff; the results are discussed further in Sec. IV C.

In the numerical solution of (23) we found it most convenient to separate the real and imaginary parts and then iterate the two coupled equations. Some care was needed in the treatment of the imaginary part of (23) because it has a trivial solution $\mathrm{Im}a(\omega)\equiv 0$. Our iteration scheme showed some tendency of being unstable towards this trivial solution; a sufficiently good starting value was usually enough to stabilize the scheme.

C. Results

We show results for parameter values $\gamma=1/256$, $\delta=1/16$, and $\gamma=\delta=1$ in Figs. 3 and 4, respectively. In Fig. 3 we show results for two different values of the cutoff parameter ($D=5$ and 8). The results are in reasonably mutual agreement but it is obvious that the cutoff in the potential *does* have some effect on the results, especially the localized level density of states seems to be sensitive to the particular choice of the cutoff. The situation is dramatically different for the case $\gamma=\delta=1$, which is obtained from the first case by making the interaction 4 times stronger keeping all other parameters fixed [see definitions of γ and δ, Eq. (24)]. As discussed above, the

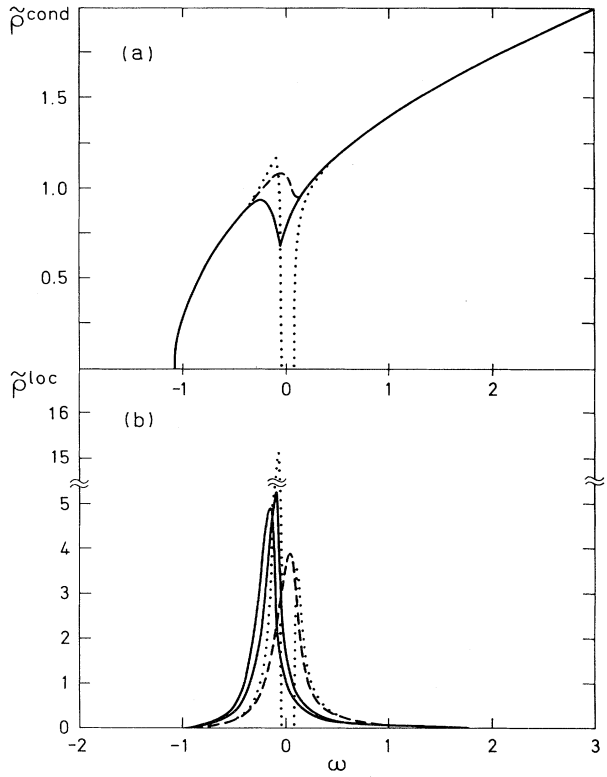

FIG. 3. (a) Conduction-electron density of state $\tilde{\rho}^{\,\mathrm{cond}}(\omega)$ and (b) the localized-level density of states $\tilde{\rho}^{\,\mathrm{loc}}(\omega)$ for weak coupling; $\delta=1/16$, $\gamma=1/256$. Solid lines correspond to a direct numerical solution for the self-consistent equation (23) for $a(\omega)$ and dashed lines represent results obtained with the analytic integration technique introduced by Pankratov. For comparison we display (the dotted line) results obtained with the erroneous self-energy used by Pankratov [Eq. (19)]. The numerical results (solid curves) were calculated with two different model interactions [Eq. (35)]: $D=5$ and 8. In the conduction-electron case the results are indistinguishable, whereas $\tilde{\rho}^{\,\mathrm{loc}}(\omega)$ peaks at a slightly lower energy for $D=8$. Note the different scales for $\tilde{\rho}^{\,\mathrm{cond}}(\omega)$ and $\tilde{\rho}^{\,\mathrm{loc}}(\omega)$ and the break in the scale for $\tilde{\rho}^{\,\mathrm{loc}}(\omega)$.

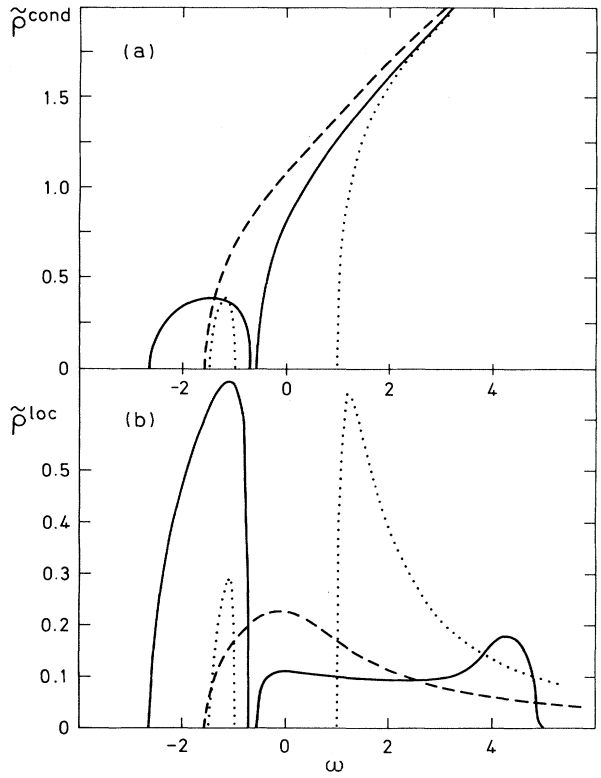

FIG. 4. (a) Conduction-electron density $\tilde{\rho}^{\,\mathrm{cond}}(\omega)$ and (b) the localized level density of states $\tilde{\rho}^{\,\mathrm{loc}}(\omega)$ for $\delta=1$, $\gamma=1$ (the interaction is 4 times stronger than in the case of Fig. 3, other parameters unchanged). Solid line represents direct numerical solution of the self-consistent equation (23) with the model interaction (35) and $D=5$. Broken line represents results for the analytical integration technique. Dots represent results for Pankratov's self-energy (19). Adding the two dotted curves leads to a total density of states which coincides with the original results shown in Fig. 6 of Ref. 9. Note the different scale for $\tilde{\rho}^{\,\mathrm{cond}}(\omega)$ and $\tilde{\rho}^{\,\mathrm{loc}}(\omega)$.

analytical method fails to yield the impurity band; the localized level electrons hybridize extremely strongly with the conduction-electron continuum. The role of the cutoff is clearly visible: It prevents the localized level electrons from "leaking out" into the conduction band, which is what happens in the Pankratov case.

For comparison, we also display in Fig. 4 Pankratov's original results. The large gap extending from $\omega=-1$ to $+1$ has nothing to do with an isolated impurity band; it results from not summing the divergent quantity $g_0(\omega)$ to infinite order when constructing the self-energy [see also the discussion following Eq. (19)]. In fact, it is easy to show[12] that the Born approximation to self-energy (19) always leads to a forbidden energy region around $\omega=0$.

V. DISCUSSION

We have evaluated the density of states for a model of a semiconductor containing a dilute concentration of resonant scatterers. The calculations are carried out for a parabolic conduction band; we use an analytical technique suggested recently by Pankratov[9] and compare the analytical results to those obtained from a direct numerical solution of the CPA-like self-consistent equations. It is found that only in the weak coupling limit are the results in reasonable agreement; the analytical method fails in the strong coupling limit because it implicitly assumes a zero-range potential and hence cannot lead to an impurity band. Therefore, we are forced to conclude that the analytical method in its present formulation seems to have only a limited range of applicability.

Analytical methods are always very useful in model calculations, and it is therefore justifiable to ask what could be done to improve the method outlined here to increase its range of validity. To our mind the largest drawback of the method is the implicit way the integral (23) appearing in the self-consistent procedure is made convergent. Hence we have sought a model interaction which would allow a more rigorous application of the contour technique. Unfortunately, we have been unable to find such an interaction. For example, the screened Coulomb interaction (25) does make the integration well defined and it is possible, in fact, to work out the residues needed in the contour calculation. Unfortunately the resulting self-consistent equation for the quantity $a(\omega)$ is extremely complicated, discouraging further work on it. A final assessment of the analytical method cannot be made before a detailed comparison is made between a numerical study and the analytical method addressing precisely the same model. It would appear to us, however, that the labor involved in the analytical method might well exceed what is needed in the numerical application.

ACKNOWLEDGMENTS

It is a pleasure to acknowledge helpful discussions with Dr. J. K. Nørskov and Dr. C. J. Pethick. The research at Cornell University was supported by the U. S. Office of Naval Research.

APPENDIX: CALCULATION OF DENSITIES OF STATES

1. Conduction electrons

The general formula for the density of states, Eq. (3), reads for the case of conduction electrons as

$$\rho(\epsilon)=-\frac{1}{\pi}\int\frac{d^3p}{(2\pi)^3}\mathrm{Im}\bar{G}(\vec{p},\epsilon)$$
$$=-\frac{1}{\pi}\frac{N(E)}{\sqrt{E}}\times\int_0^\infty d\epsilon_k\sqrt{\epsilon_k}\,\mathrm{Im}\left[\frac{1}{\epsilon-\epsilon_k-\mathrm{Re}\Sigma(\epsilon)+i\,\mathrm{Im}\Sigma(\epsilon)}\right]. \quad \text{(A1)}$$

In (A1) we have explicitly indicated that the retarded Green function has a pole in the lower half of the complex energy plane. The integral in (A1) is evaluated along the

contour shown in Fig. 1 and the result is

$$\rho(\epsilon)=\frac{N(E)}{\sqrt{E}}\frac{1}{2}\{[\epsilon-\mathrm{Re}\Sigma(\epsilon)+i\,\mathrm{Im}\Sigma(\epsilon)]^{1/2} -[\epsilon-\mathrm{Re}\Sigma(\epsilon)-i\,\mathrm{Im}\Sigma(\epsilon)]^{1/2}\ . \tag{A2}$$

It is important to notice that the branch cut of the square-root function was placed on the positive real axis (see Fig. 1). Hence the phase angles of all complex numbers are restricted to the range $[0,2\pi]$. Thus (A2) is of the form

$$\rho(\epsilon)=\frac{N(E)}{2\sqrt{E}}\sqrt{r}\,(e^{i\Phi/2}-e^{i(2\pi-\Phi)/2})=\frac{N(E)}{\sqrt{E}}\sqrt{r}\,\cos(\Phi/2)\ , \tag{A3}$$

where

$$r=\{[\epsilon-\mathrm{Re}\Sigma(\epsilon)]^2+[\mathrm{Im}\Sigma(\epsilon)]^2\}^{1/2}$$

and

$$\Phi=\tan^{-1}\left[\frac{\mathrm{Im}\Sigma(\epsilon)}{\epsilon-\mathrm{Re}\Sigma(\epsilon)}\right]\ . \tag{A4}$$

A simple trigonometric calculation with (A3) and (A4) then gives

$$\rho(\epsilon)=\frac{N(E)}{\sqrt{2E}}(\epsilon-\mathrm{Re}\Sigma(\epsilon) +\{[\epsilon-\mathrm{Re}\Sigma(\epsilon)]^2+[\mathrm{Im}\Sigma(\epsilon)]^2\}^{1/2})^{1/2}\ , \tag{A5}$$

which is Eq. (32) used in the text (recall that $\omega=\epsilon/E-1$). Observe that as the interaction is turned off [i.e., $\Sigma(\epsilon)\to 0$] (A5) reduces to the free-electron value $\rho(\epsilon)=N(\epsilon)$, as it should. It is also seen that for large negative values of ϵ for which $\mathrm{Im}\Sigma(\epsilon)$ vanishes (A5) also vanishes, provided that $\epsilon-\mathrm{Re}\Sigma(\epsilon)<0$.

2. Localized level density of states

The form of (3) appropriate for the localized levels is

$$\rho_{\mathrm{loc}}(\epsilon)=-\frac{1}{\pi}\frac{1}{\Omega}\sum_{\alpha}\mathrm{Im}g(\alpha,\alpha;\epsilon)\ . \tag{A6}$$

In our calculation we have [see Eqs. (10) and (17)]

$$g(\alpha,\alpha;\epsilon)=\frac{1}{g_0^{-1}(\epsilon)-\sum_{\vec{k}}|V(\vec{k})|^2\bar{G}(\vec{k},\epsilon)}\ , \tag{A7}$$

from which we get [note that $c/E\pi=\frac{1}{2}N(E)\delta/\sqrt{\gamma}$]

$$\tilde{\rho}_{\mathrm{loc}}(\omega)=\frac{1}{2}\frac{\delta}{\sqrt{\gamma}}\frac{\mathrm{Im}a(\omega)}{[\omega-\mathrm{Re}a(\omega)]^2+[\mathrm{Im}a(\omega)]^2}\ , \tag{A8}$$

For a numerical example, see the discussion in Sec. IV.

[1]P. W. Anderson, Phys. Rev. 124, 41 (1961).

[2]J. Friedel, Can. J. Phys. 34, 1190 (1956); Nuovo Cimento Suppl. 7, 287 (1958).

[3]M. Salomaa, Z. Phys. B 25, 49 (1976); M. Salomaa and R. Nieminen, Z. Phys. B 35, 15 (1979).

[4]M. J. Zuckerman, Phys. Rev. 140, A899 (1965).

[5]D. M. Newns, Phys. Rev. 178, 1123 (1969).

[6]J. K. Nørskov, J. Vac. Sci. Technol. 18, 420 (1981).

[7]K. Schönhammer and O. Gunnarsson, Phys. Rev. B 22, 1629 (1980).

[8]A. P. Jauho, J. W. Wilkins and F. P. Esposito, J. Phys. (Paris) Colloq. 42, C7-301 (1981); A. P. Jauho, Ph.D. thesis, Cornell University, 1982 (unpublished); A. P. Jauho and J. W. Wilkins, Phys. Rev. Lett. 49, 762 (1982).

[9]O. A. Pankratov, Fiz. Tverd. Tela (Leningrad) 23, 68 (1981) [Sov. Phys.—Solid State 23, 38 (1981)].

[10]R. J. Elliot, J. A. Krumhansl, and P. L. Leath, Rev. Mod. Phys. 46, 465 (1974).

[11]The authors are grateful to Dr. J. K. Nørskov for this argument.

[12]The proof is based on the observation that Eq. (29) with the Pankratov self-energy (19) (i.e., $\delta/[\omega-a(\omega)]\to\delta[1/\omega+a(\omega)/\omega^2]$) always leads to a *real* $a(\omega=0)$, i.e., to a vanishing imaginary part of the Green function.